Thin Solid Films 785 (2023) 140092

Contents lists available at ScienceDirect

Thin Solid Films

journal homepage: www.elsevier.com/locate/tsf

Influence of processing conditions on the titanium/nickel contact metallization on a silicon wafer for thermal management

Manish Singh [1], Lakshmi Narayanan Ramasubramanian, Raj N. Singh [*]

School of Materials Science and Engineering, Oklahoma State University, 700 N. Greenwood Avenue, Tulsa, Oklahoma 74106, USA

ARTICLE INFO

Keywords:
Silicon
Titanium
Nickel
Thin film
Direct current magnetron sputtering
Diamond
Thermal management

ABSTRACT

Thermal management of both digital and power electronics is becoming challenging with device miniaturization and a need for delivering higher power. Diamond thin films and substrates are attractive for thermal management applications in power electronics because of their high thermal conductivity. However, deposition of diamond by microwave plasma enhanced chemical vapor deposition requires high temperatures, which can degrade metallization used in power electronic devices. In this research, Titanium (Ti)- Nickel (Ni) thin films are deposited by direct current magnetron sputtering on p-type Silicon (Si) (100) substrates using a physical mask for creating dot-patterns for measuring properties of the contact metallization. The influence of processing conditions and post-deposition annealing in Argon and hydrogen at 380 °C for 1 h on the properties of the contact metallization are studied by measuring the current - voltage characteristics and Hall effect. The results indicated ohmic contact resistance for both, the as-deposited films and after post annealing treatments. In addition, the results on contact resistance, resistivity, carrier concentration and hall mobility of wafers extracted from Ti/Ni metal contact to p-type Si (100) are presented and discussed.

1. Introduction

Since the last decades, the increasing demand for miniaturization of electronic devices has created huge interest in research on thin film technology [1–7]. Thin films of metals or their alloys, such as copper (Cu), nickel (Ni), aluminum (Al) or Titanium (Ti)-Cu, Ti-Ni, Ti-Al, exhibit varied mechanical, electrical, chemical, or magnetic properties and have been used for the metallization in microelectronic devices [1–3,8–11]. For example, Cu thin films on semiconductor substrate have shown properties such as high conductivity, good electromigration resistance and high melting point, which make them suitable candidate for interconnection [2,12,13]. Also, fabrication of Ni-based thin film materials possess good corrosion and wear resistant and have gathered attention in broad range of applications from contact metallization of micro devices to lithium-based energy storage materials [14]. Furthermore, the unique properties of metal alloys of Ti-Ni and thin films are of scientific interest in micro-electro-mechanical systems. These alloys have properties like good corrosion resistance, biocompatibility, pseudo elasticity, damping capacity, and shape memory effect [8,15–18].

To fabricate thin films, plasma-assisted techniques such as plasma-enhanced chemical vapor deposition, physical vapor deposition alone or in combination with laser ablation, plasma etching, ion beam etching/deposition, and reactive ion etching are widely used in microsystems and semiconductor technology. For instance, magnetron sputtered nanocrystalline Ni films deposited on silicon (Si) substrates function as a solar absorber in solar cell [5]. There are various routes to fabricate Ni–Ti based thin alloy film on Si substrate by sputter deposition technique [17,19,20]. These include deposition either by sputtering from Ni–Ti alloy targets or by co-sputtering from elemental Ni and Ti targets on the Si substrates. Ni/Au films are also used as interconnect metallization in GaN-based power and microwave electronics [21–27].

Si based high-power electronics device have been used in high-frequency circuit applications for the last few decades. Si based devices can be operated at high-temperatures and high-power levels. In addition, as electronics feature become smaller, their high-power density and high heat flux density cause an increase in temperature, which can result in poor performance and a shortened lifespan. Various kinds of high-power electronics are being used in extreme environment conditions, such as high temperature and high-pressure where performance degradation and operational failure are more likely to occur for

* Corresponding author.
E-mail address: rajns@okstate.edu (R.N. Singh).
[1] Present address: Department of Metallurgical and Materials Engineering, Indian Institute of Technology Patna, Bihta, Bihar 801106, India.

https://doi.org/10.1016/j.tsf.2023.140092
Received 18 February 2023; Received in revised form 20 October 2023; Accepted 21 October 2023
Available online 23 October 2023

Table 1
A summary of DC magnetron sputtering conditions used for Ti and Ni depositions sequentially.

Metal target	Pressure (Pa)	Power (Watts)	Deposition Time (min) /Thickness (μm)
Titanium (Ti)	0.4	50	5 min/.01 μm
Nickel (Ni)	0.4	300	45 min/ 1 μm

electronics. High current densities in semiconductor electronics operating at high power levels result in significant self-heating of devices, which necessitates the development of thermal management technologies to effectively dissipate the generated heat. To improve the heat dissipation, materials with high thermal conductivity and low thermal expansion are needed [18–24]. Diamond is being explored because of these attributes but requires effective metallization such as Ni/Ti described in this paper.

Therefore, it is important to create effective thermal management strategies for Si-based power electronics or high-power electronics devices [28–30]. In this context, thin film diamond is being used as an attractive material for thermal management of semiconductor electronics owing to its outstanding optical, electrical, mechanical, and thermal properties [30]. Diamond has high thermal conductivity, a large band gap and a large breakdown electric field. Also, Diamond is an electrical insulator but at the same time it is an excellent thermal conductor, which is being explored to remove heat generated in electronic devices.

Among the numerous diamond deposition processes, the hot filament chemical vapor deposition (HFCVD) process and the microwave plasma enhanced chemical vapor deposition (MPECVD) methods have proven to be the most widely used diamond deposition processes for producing high-quality diamond films. However, high temperature diamond synthesis comes with limitations, so for electronics device, low temperature diamond synthesis (<400 °C) is desirable. Low temperature diamond thin film or nanocrystalline diamond synthesis methods using MPECVD or HFCVD methods on Si based power electronics require temperature below 400 °C [30,31]. However, it is still unclear from the literature whether the metallization of the device will be degraded by the deposition of a diamond thin film on Si. Our team has conducted research on the processing of diamond thin films for thermal management of GaN-based power electronics with Ni/Au metallization at temperatures below 400 °C [21–27].

Nickel metallization of silicon is considered a valuable method for semiconductor device fabrication [9,32]. Numerous reports on nickel silicide formation in the metallized layer after annealing nickel-metallized silicon at 200 °C–325 °C can be found in the literature [33,34]. Diffusion barriers like titanium, vanadium, molybdenum, titanium nitride etc. are utilized to prevent interdiffusion between layers of doped silicon and metal metallization [35–38]. A thin diffusion layer between nickel and silicon would prevent the formation of nickel silicide at temperatures lower than 400 °C. Titanium thin films have been used as a successful diffusion barrier as well as an adhesion promoter in semiconductor technology due to their characteristic properties, such as high thermal and chemical stability as well as low electrical resistivity. We have selected Ti/Ni for contact metallization on Si for application in power electronics where diamond can serve as heat spreader for thermal management.

When evaluating electrical characteristics of semiconductor materials, such as resistivity, carrier concentration/density, and hall mobility, the Van Der Pauw method is one of the techniques that has been used the most in the literature [39–41]. It can be used to measure samples of arbitrary shape, although few basic assumption of sample conditions must be satisfied to obtain accurate measurements such as the thickness of the measured sample must be constant (and less than 1 mm), point contacts placed at the edges of the samples must be used for the measurements, and the sample should be homogeneous with no hole. Most semiconductor samples satisfy these conditions. Therefore, this approach is widely utilized in semiconductor technologies.

The main objectives of this paper are processing and measuring electrical properties of Ti/Ni metal contact on Si. The processing was carried out using a sputtering technique, and Hall measurements in a Van Der Pauw configuration were used to determine the electrical properties at room temperature. The results were analyzed for determining the nature of the metal-Si contact resistance from current (I)-voltage (V) data, and resistivity, career concentration, Hall mobility and Hall coefficient of the Si substrate. In addition, Ti/Ni metal contact on Si were subjected to post annealing treatments in Ar and H_2 atmospheres at 380 °C for 1 h (typical for diamond deposition as heat spreader), and the I-V characteristic and electronic properties were determined and discussed after post annealing in Ar and H_2 environments.

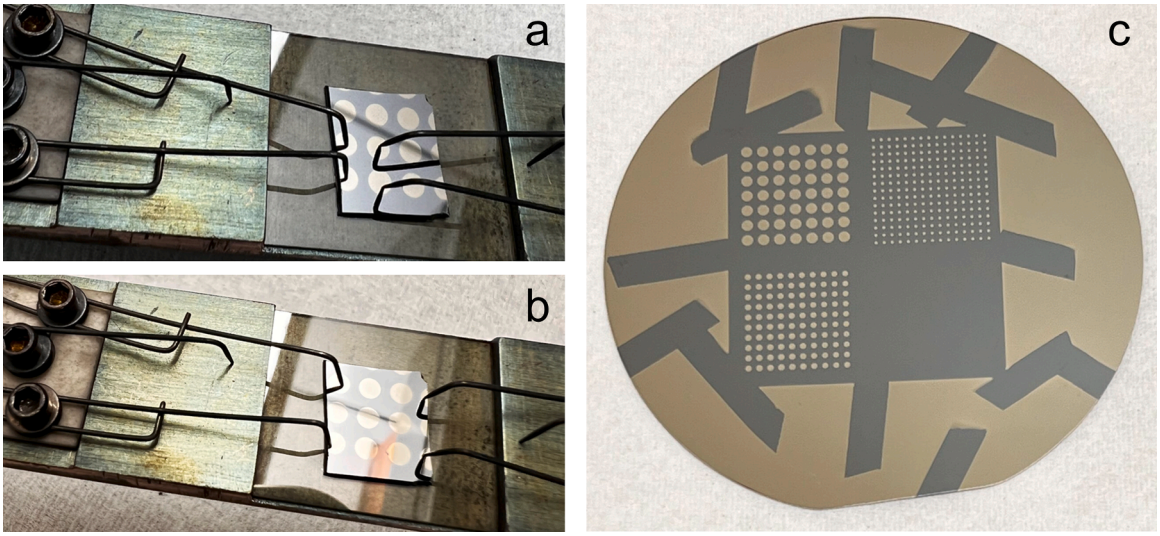

Fig. 1. Photographs Showing Ti/Ni type I contact on p-Si (100) of (a) the continuous contact dot pattern and (b) corner contact dot pattern. Photograph in (c) Ti/Ni dots of different diameters deposited on p-Si (100) wafer. Ti/Ni contact type I (2 mm), type II (1 mm), type III (0.5 mm) and type IV (0.05 mm) are defined based on the diameter of the circular dot.

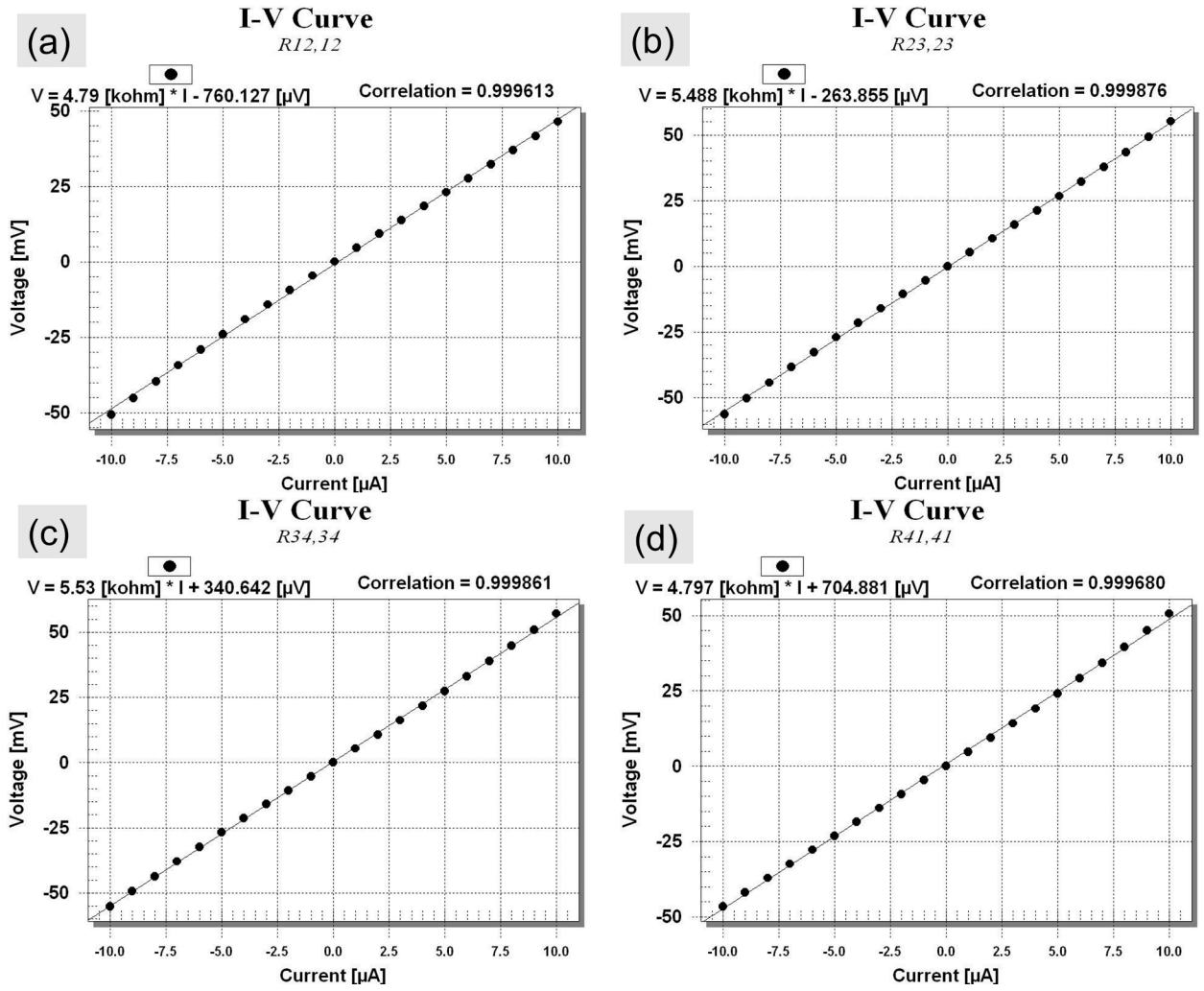

Fig. 2. I-V characteristics of Ti/Ni continuous contact of type I on Si (100) in the as-deposited state between contacts (a) 1-2, (b) 2-3, (c) 3-4, and (d) 4-1.

2. Materials and methods

2.1. Deposition of Ti/Ni metal contacts on Si (100) wafer using a metal mask

Ti and Ni films were sequentially sputtered on p-type Si (100) wafer substrate using Direct current (DC)-magnetron sputtering system (Model # ATC ORION 8 Sputtering System from AJA INTERNATIONAL, Inc.), which is a five-gun system. DCXS-750-4 Multiple Sputter Source DC Power Supply was used as sputtering power supply. The sputter chamber was evacuated to a base pressure lower than $<1.33 \times 10^{-5}$ Pa using turbo molecular pump and a rotary pump. Ni and Ti targets (99.9 % pure) of diameter of 2″ and thickness 0.25″, respectively, were employed as the sputter target. The Argon (Ar) gas (of 99.9 % purity) was used as the sputtering gas with a constant flow rate of 20 sccm. The chamber pressure was measured by ion-gauge and the Ar gas pressure was controlled by the throttle valve. Before deposition, p-type Si (100) substrate was ultrasonically cleaned with acetone for 5 min and rinsed with water. Then, it was ultrasonically etched with 5 % Hydrofluoric acid for 5 min followed by rinsing with water and isopropyl alcohol to remove native oxide layer from the Si surface.

Pre-sputtering of Ti and Ni targets was carried out in order to ensure the purity of the films. The surface of the Ti and Ni targets was cleaned using pre-sputtering with pure Ar. Pre-sputtering for Ti and Ni targets took place for a total of 5 min, with pre-sputtering powers of 50 W and 300 W, respectively. Also, sputtering power was slowly increased by 50 W/10 s when the Ti and Ni targets were pre-sputtered. In addition, there was good circulation of cooling water to ensure continuous sputtering with high power without the interruption.

Substrates were rotated at 20 rpm during deposition for uniformity. Ti and Ni films were sequentially deposited at the same deposition pressure (Pa), different DC sputtering power (W) and different deposition time (min) as mentioned Table 1. Working distance between target and substrate of 20 cm was used for all depositions. Also, a 2″ x 2″ mask was placed on top of the 4” diameter Si (100) wafer before sputtering. Since Ni is a magnetic material, it required a different setup for sputtering to ensure plasma formation and good deposition rates. The Ti target did not require any special setup because it is non-magnetic. We used very thin Ti layer (~ 0.01 μm) for ensuring good adhesion to Si substrate followed by deposition of a relatively thicker Ni film (~ 1 μm .

2.2. Characterization of Ti/Ni contact on Si (100) substrate using Van der Pauw method

Before I-V and Hall measurements, smaller samples approximately ~1″ x 1″ were obtained from a larger Ti/Ni deposited on the p-Si (100) (Fig. 1c) by cleaving into 4 parts and named as Ti/Ni contact type I, type II, type III, and type IV, depending on the circular dot size of the contact. Contact type I refers to bigger dot type and contact type IV refers to smallest contact type. For this paper, Ti/Ni contact type I was used and explored. To measure I-V characteristics and Hall measurements, Ti/Ni contact type I was broken into 4 square shape samples ~ 1 cm x 1 cm,

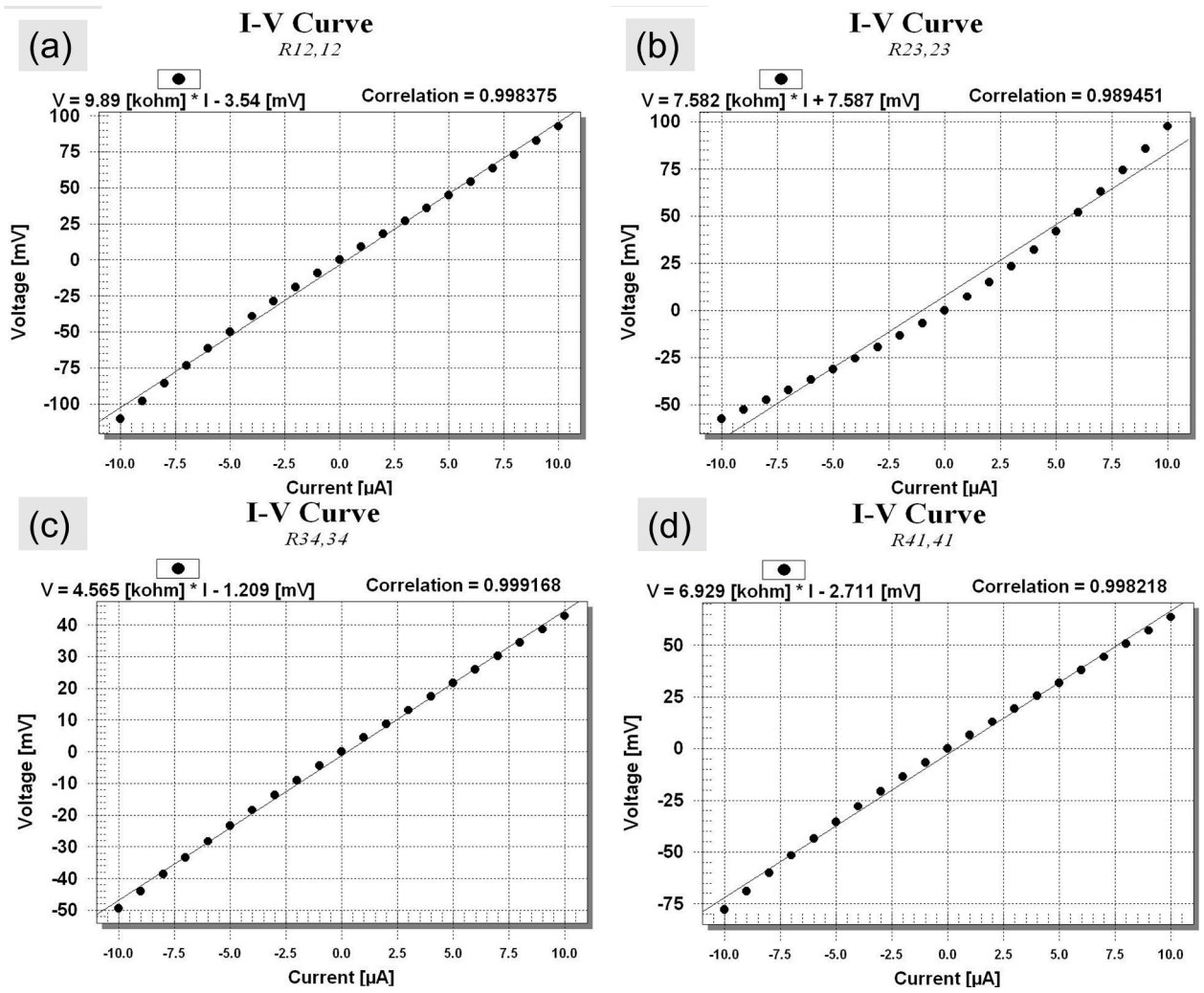

Fig. 3. I-V characteristics of Ti/Ni corner contact of type I on Si (100) in the as-deposited state between contacts (a) 1-2, (b) 2-3, (c) 3-4, and (d) 4-1.

and each square sample was used for measurements. Also, to measure Ti/Ni contact type I, two different approaches were considered, first is the continuous contact and second is the corner contact as shown in Fig. 1a, b. To measure I-V characteristics, initial current of -10 µA was applied. Final current was set to 10 µA and step current used was 1 µA.

The electrical properties of the Ti/Ni type I contact were studied using Hall effect measurement system from Lake Shore Cryotronics, Inc. in the Van der Pauw configuration at room temperature from which resistivity, Hall coefficient and Hall mobility were calculated. Si samples of thickness 500 µm was used to carry out the Hall measurements. For variable magnetic field measurement, linear sweep field reversal was selected, maximum and minimum fields were 250 mT and 50 mT, respectively. The field step used was 50 mT and a constant current of 10 µA was applied to the Ti/Ni type I contact on Si (100).

2.3. Annealing procedures

Post annealing of Ti/Ni films deposited on p-Si (100) substrate was performed in a tube furnace. Ti/Ni films were annealed at 380 °C under Ar atmosphere. Ti/Ni film on Si substrate was placed in a quartz boat at the central zone of the horizontal 3-zone tube furnace. The furnace was evacuated to 10^{-5} Pa and purged by using N_2. Then, the system was evacuated to 10^{-5} Pa and purged with Ar to reach atmospheric condition (760 torr). The sample was heated to 380 °C for 1 h in a flowing Ar atmosphere at a flow rate of 20 sccm. Then, the furnace was cooled down in the Ar cover gas. Another set of Ti/Ni samples were annealed at 380 °C under pure hydrogen (H_2) atmosphere following similar steps. The annealed samples were characterized for electrical properties as well.

3. Results and discussion

Ti/Ni metal contacts on p-Si (100) were processed and the properties of these contacts were determined using I-V and Hall measurements as described earlier and the results are presented and discussed in the following sections.

3.1. Current-Voltage (I-V) behaviors of Ti/Ni type I metal contact on p-Si (100)

After DC magnetron sputtering Ti/Ni metal contacts in the form of dot patterns are obtained on p-Si (100) wafer as shown in Fig. 1c. As mentioned earlier first a thin Ti layer (adhesion promoter) is deposited followed by a thicker Ni layer. The I-V measurements used type-I contact of 2 mm diameter on samples in the as-deposited state and after annealing in Ar or H_2 at 380 °C for 1 h.

The results for samples in the as-deposited state are given in data of Fig. 2 and Fig. 3, respectively, for the continuous and corner contacts measured between 1-2, 2-3, 3-4 and 4-1 probe locations. Fig. 2 (a-d) show almost linear I-V response with the correlation coefficient slightly less than 1 indicating almost ohmic contact measured on continuous dot pattern. The results obtained for the corner contacts are given in Fig. 3

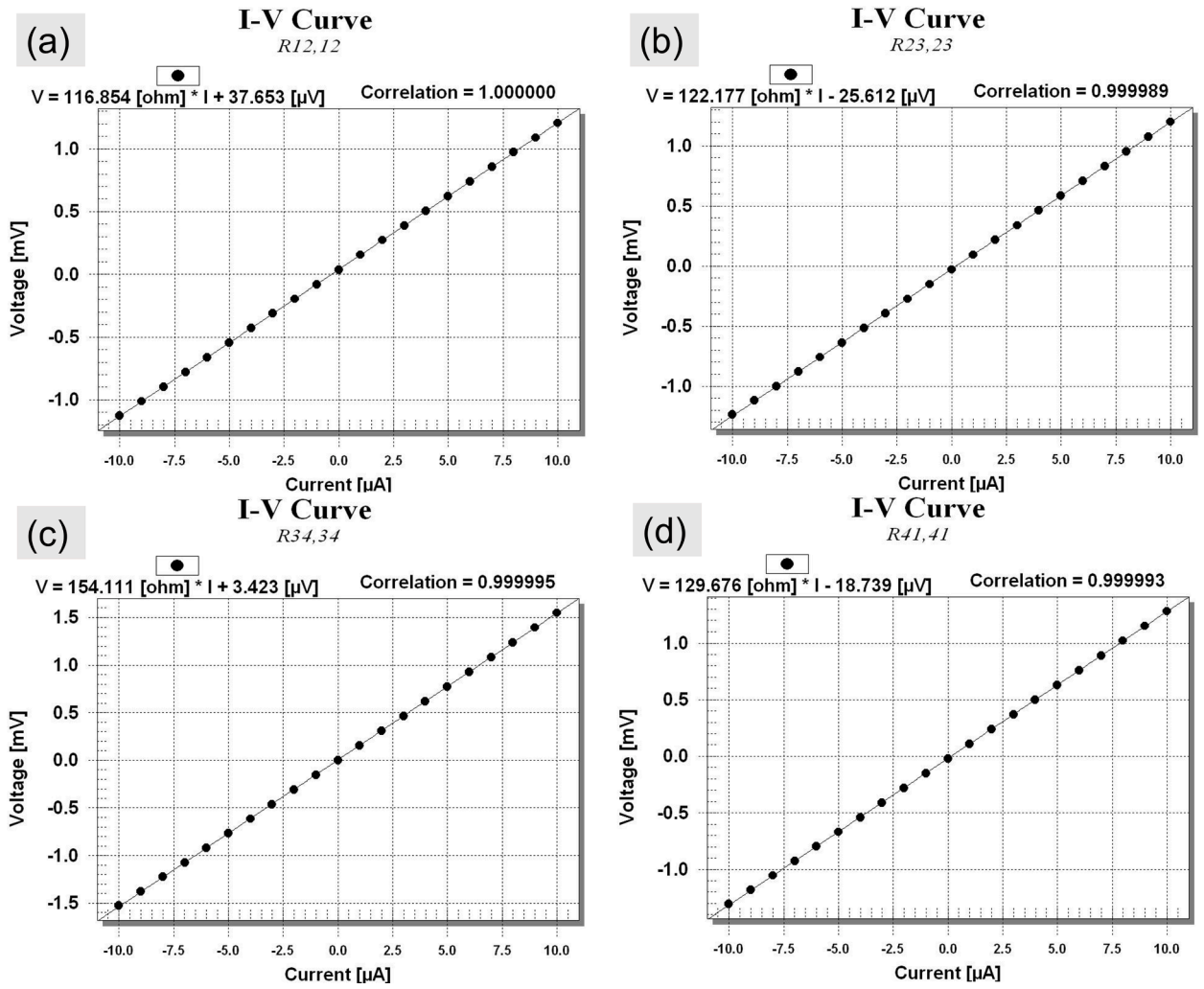

Fig. 4. I-V characteristics of Ti/Ni continuous contact of type I on Si (100) after annealing in Ar at 380 °C for 1 h between contacts (a) 1-2, (b) 2-3, (c) 3-4, and (d) 4-1.

(a-d) and show more non-linear response than the data of Fig. 2. This is most likely a result of not well-formed contacts created upon cleaving smaller samples for the measurements. This indicated that continuous contacts may be more appropriate for I-V characterization.

The Ti/Ni samples deposited on p-Si (100) were then annealed in the Ar atmosphere at 380 °C for 1 h and I-V characteristics were measured in a manner similar to the as-deposited samples. The results are given in Fig. 4 and Fig. 5, respectively, for the continuous and corner contacts. All the I-V curves show linear responses and the correlation coefficient approaching very close to 1. These results indicated that the ohmic contacts of Ti/Ni on Si can be readily made after a low-temperature annealing in an inert Ar atmosphere.

Ti was applied to p-Si (100) as a diffusion barrier and an adhesion promoter. For the Ti-Si system, due to the use of room-temperature DC magnetron sputtering, Ti shouldn't diffuse into p-Si (100) in the as-deposited state. Also, Energy-dispersive X-ray did not show any diffusion after annealing at 380 C in the Ar/H2 atmosphere within the detectability limits (data not shown). So, significant Ti-Si reaction should not occur during annealing at low temperature of 380 °C, while some intermixing may be possible to promote adhesion and ohmic contact formation. For the Ti-Ni system, literature showed amorphization of the Ti/Ni layers after annealing at temperatures between 200 °C and 330 °C [42,43]. At relatively low temperatures (200–300 °C), it has been found that amorphization results from faster Ni atom diffusion into Ti layers. It is significant to note that intermetallic $TiNi_3$ and Ti_2Ni alloy phases are more likely to form in the Ni-Ti system after annealing at temperatures above 500 °C [44]. Both of the constituent elements involved must diffuse for the Ti-Ni intermetallic compound to form. So, at higher temperatures, Ni and Ti diffuse into one another, forming intermetallic Ti-Ni nucleation sites at the interface [44]. Since our annealing temperature is low, we do not expect intermetallic formation or significant interdiffusion.

Similarly, I-V characteristics were measured after annealing the Ti/Ni samples deposited on Si(100) wafers in pure H_2 gas at 380 °C for 1 h. Both the continuous and corner contacts were investigated, and the results are shown in Fig. 6 and Fig. 7, respectively, for the continuous and corner contacts. The results show purely ohmic contact resistance for all H_2-annealed samples, which are similar to post annealing treatment in Ar atmosphere as well. These I-V behaviors indicated that essentially ohmic contact resistance can be readily obtained for Ti/Ni contacts on p-Si (100) by annealing preferably in H_2 atmosphere at low temperatures.

3.2. *Characterization of properties of p-Si (100) using Ti/Ni metal contact through Hall measurement*

The Hall measurement was done using the Ti/Ni contact metallization as described in the previous sections. This approach utilized the Van der Pauw configuration (dot-pattern) to measure properties of the p-Si (100) substrate. All measurements were done at room temperature at different applied magnetic fields and on continuous and corner dot

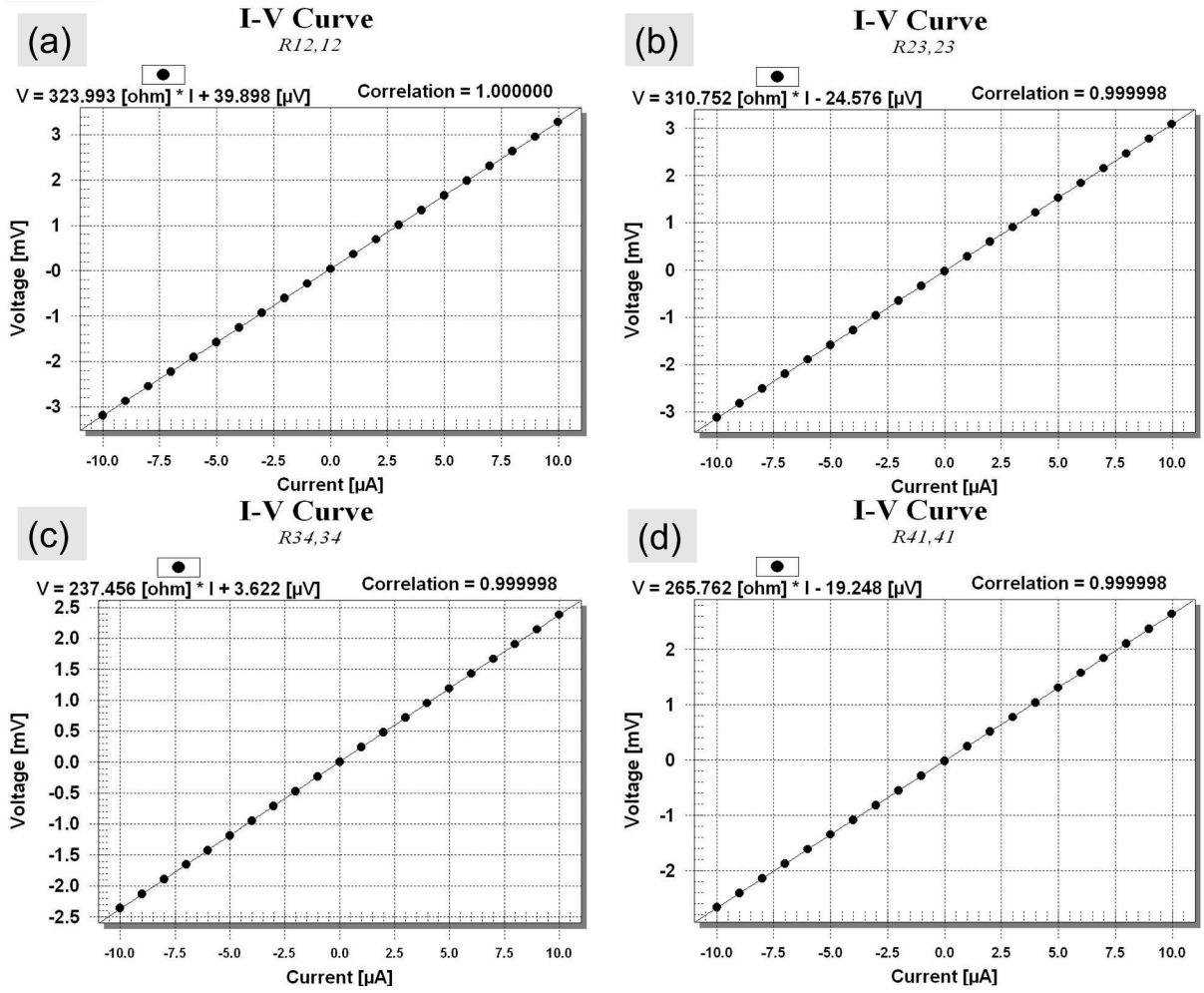

Fig. 5. I-V characteristics of Ti/Ni corner contact of type I on Si (100) after annealing in Ar at 380 °C for 1 h between contacts (a) 1-2, (b) 2-3, (c) 3-4, and (d) 4-1.

patterns. From these measurements, resistivity, carrier concentration, and Hall mobility of the p-Si(100) were obtained. The following equations describe how these properties were measured automatically using software as a part of the Lake Shore Hall instrument.

To measure resistivity using Van der Pauw method, four contact points are used as shown in Fig. 8a for Ti/Ni corner contact of type I on Si (100). The procedure for measuring resistivity requires two resistance measurements. For instance, the current source is connected between contacts 2 and 1 and the voltage is measured between contacts 3 and 4. The current is reversed to remove thermoelectric voltages and a current reversed resistance is measured. This is denoted as $R_{21,34}$. The current source and voltmeter are rotated to source the current between contacts 3 and 2 and the voltage is measured between contacts 4 and 1. The current is reversed again to remove thermoelectric voltages to obtain a current reversed resistance $R_{32,41}$

$$R_{21,34} = \frac{V_{34}\left(I_{21}^{+}\right) - V_{34}\left(I_{21}^{-}\right)}{I_{21}^{+} - I_{21}^{-}} \tag{1}$$

$$R_{32,41} = \frac{V_{41}\left(I_{32}^{+}\right) - V_{41}\left(I_{32}^{-}\right)}{I_{32}^{+} - I_{32}^{-}} \tag{2}$$

These two resistance readings are converted to a resistivity by solving the non-linear equation for the factor "f" to calculate the resistivity. This measured resistivity is the sheet resistivity.

$$\rho_{sheet}^{A} = \frac{\pi f\left(R_{21,34} + R_{32,41}\right)}{\ln(2)2} \tag{3}$$

Here f is the solution to the equation.

$$\frac{q-1}{q+1} = \frac{f\,cosh^{-1}\left(\frac{\frac{ln2}{e^{f}}}{2}\right)}{\ln(2)} \tag{4}$$

where

$$q = \frac{R_{21,34}}{R_{32,41}}\ or\ q = \frac{R_{32,41}}{R_{21,34}}\ which\ ever\ is\ larger$$

Similarly, resistance $R_{43,12}$ and $R_{43,12}$ are obtained by considering other current and voltage contacts as shown in Fig. 8b,

$$R_{43,12} = \frac{V_{12}\left(I_{43}^{+}\right) - V_{12}\left(I_{43}^{-}\right)}{I_{43}^{+} - I_{43}^{-}} \tag{5}$$

$$R_{14,23} = \frac{V_{23}\left(I_{14}^{+}\right) - V_{23}\left(I_{14}^{-}\right)}{I_{14}^{+} - I_{14}^{-}} \tag{6}$$

$$\rho_{sheet}^{B} = \frac{\pi f\left(R_{21,34} + R_{32,41}\right)}{\ln(2)2} \tag{7}$$

Here f is the solution to the equation.

$$\frac{q-1}{q+1} = \frac{f\,cosh^{-1}\left(\frac{\frac{ln2}{e^{f}}}{2}\right)}{\ln(2)} \tag{8}$$

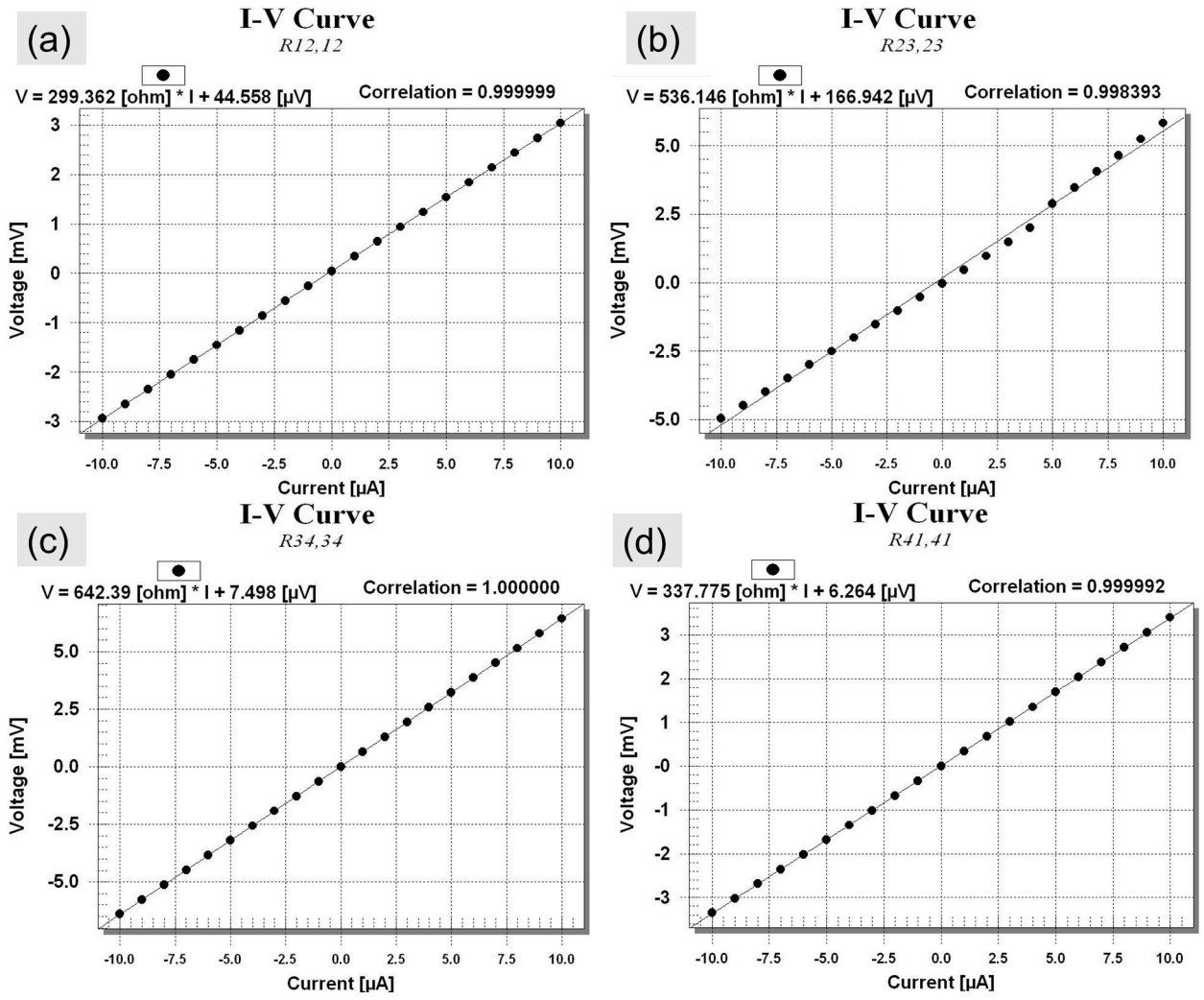

Fig. 6. I-V characteristics of Ti/Ni continuous contact of type I on Si (100) after annealing in H_2 at 380 °C for 1 h between contacts (a) 1-2, (b) 2-3, (c) 3-4, and (d) 4-1.

where

$$q = \frac{R_{43,12}}{R_{14,23}} \; or \; q = \frac{R_{14,23}}{R_{43,12}} \; which \; ever \; is \; larger$$

Thus, the final sheet resistivity is given by

$$\rho = \frac{\rho^{A}_{sheet} + \rho^{B}_{sheet}}{2} \tag{9}$$

$$\rho_{bulk} = \rho_{sheet} * t \tag{10}$$

$$Resistivity = \rho_{bulk} = \rho_{sheet} * t$$

where t is the thickness of Si.

Further, to measure Hall voltage using Van der Pauw method, current source is connected across the diagonal of the sample and the voltage is measured across the other diagonal (see Fig. 8c). The voltage is measured at both positive and negative fields as well as positive and negative currents to eliminate misalignment voltages thereby resulting in four separate measurements. These four measurements are then used to calculate the Hall voltage, V_{Hall}.

For the current source applied between contact 3 and 1 as shown in Fig. 8c (left figure),

$$V^{B+}_{13,42} = \frac{V^{B+}_{42}(I^{+}_{13}) - V^{B+}_{42}(I^{-}_{13})}{2} \tag{11}$$

$$V^{B-}_{13,42} = \frac{V^{B-}_{42}(I^{+}_{13}) - V^{B-}_{42}(I^{-}_{13})}{2} \tag{12}$$

$$V_{AHall} = \frac{V^{B+}_{13,42} - V^{B-}_{13,42}}{2} \tag{13}$$

Similarly, when current source is applied between contact 2 and contact 4 as show in Fig. 8c (right figure),

$$V^{B+}_{24,31} = \frac{V^{B+}_{31}(I^{+}_{24}) - V^{B+}_{31}(I^{-}_{24})}{2} \tag{14}$$

$$V^{B-}_{24,31} = \frac{V^{B-}_{31}(I^{+}_{24}) - V^{B-}_{31}(I^{-}_{24})}{2} \tag{15}$$

$$V_{BHall} = \frac{V^{B+}_{24,31} - V^{B-}_{24,31}}{2} \tag{16}$$

$$V_{Hall} = \frac{V_{AHall} + V_{BHall}}{2} \tag{17}$$

The V_{hall} is related to the fundamental properties as,

$$V_{Hall} = \frac{IB_z}{nqt} \tag{18}$$

where, n is the carrier density, t is the thickness of sample, q is the

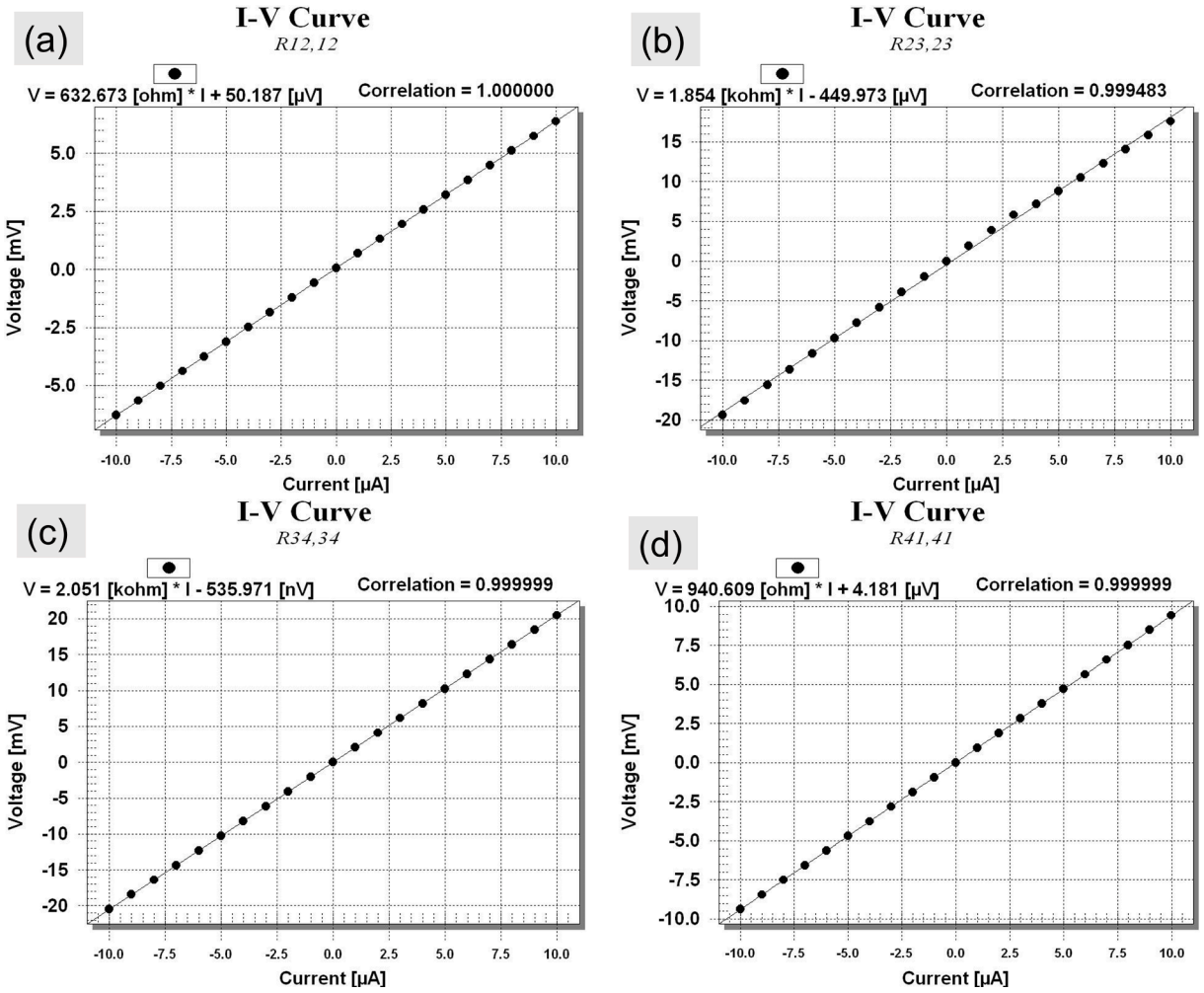

Fig. 7. I-V characteristics of Ti/Ni corner contact of type I on Si (100) after annealing in H_2 at 380 °C for 1 h between contacts (a) 1-2, (b) 2-3, (c) 3-4, and (d) 4-1.

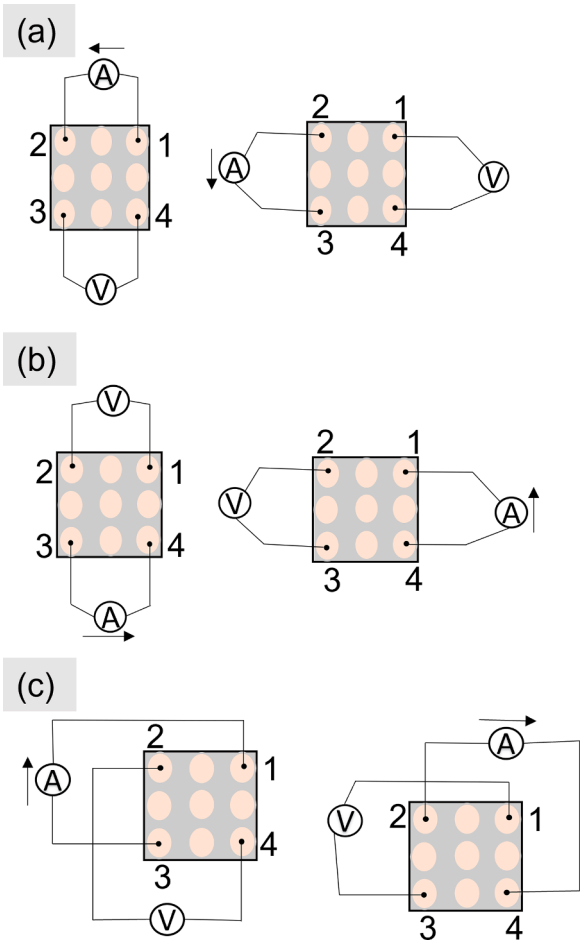

Fig. 8. (a) The Van der Pauw sample of Ti/Ni with corner contacts of type I on p-Si (100) showing the connections for resistivity measurements. (b) A second set of contacts for measuring Van der Pauw resistivity of Ti/Ni corner contact of type I on p-Si (100). (c) The configurations for measuring Hall voltage of Ti/Ni corner contact of type I on p-Si (100) using Van der Pauw method.

electronic charge, B_Z is the magnetic field, and I is the current.

The Hall coefficient, $R_{H,}$ can be expressed as,

$$R_H = \frac{V_{Hall}t}{IB_z} \tag{19}$$

After we measure the resistivity and Hall coefficient, then the carrier concentration and Hall mobility can be obtained from the following equations,

$$Carrier\ concentration = n = \frac{1}{qR_H} \tag{20}$$

$$Hall\ mobility = \mu = \frac{1}{\rho nq} = \frac{R_H}{\rho} \tag{21}$$

where n, μ, ρ, R_H, q represents the carrier concentration, Hall mobility, resistivity, Hall coefficient and carrier charge, respectively.

The electrical properties of the Ti/Ni type I contact on Si (100) were determined and the results for the continuous and corner contacts are presented in Fig. 9a and 9b, respectively. The resistivity, carrier concentration and Hall mobility are found to be independent of the applied magnetic field for all samples tested. Typical values for the Ti/Ni type I continuous contact, in the as-deposited state, on Si are 1×10^{22} m^{-3} for the carrier concentration, 0.011 m^2/V-s for the carrier mobility, and 5.64 ohm-cm for the resistivity as presented in Fig. 9. There is only a small change to these values when comparing the as deposited and annealed (Ar and H_2) samples. Similarly, for the Ti/Ni type I corner contacts, in the as-deposited state, the electrical properties were measured (Table 2) as carrier concentration of 2.4×10^{21} m^{-3}, carrier mobility of 0.0325 m^2/V-s, and resistivity of 8.45 ohm-cm. Also, a comparison of the as fabricated and annealed (Ar and H_2) samples shows similar resistivity, carrier concentration and carrier mobility values.

A summary of all measured properties of Ti/Ni metal contacts on Si (100) is given in Table 2. After being annealed in the atmospheres of Ar or $H_{2,}$ its properties barely changed. However, earlier I-V data are much more confirmative on whether the contacts are purely ohmic with high degree of confidence. It also confirms that annealing at high temperature of 380 °C for 1 h did not change the electrical properties, especially the contact resistance remained ohmic with values similar to the samples in the as-deposited state. Also, the properties of p-Si (100) wafer extracted from this study are similar to the range of values supplied by the vendor of the wafers (thickness- 500 μm, *p*-type, doping level of boron in Si (100) is 0.74×10^{21} - 1.67×10^{22} m^{-3}. Also, mobility and resistivity are in the range of 0.0368-0.0418 m^2/V-S and 1-20 ohm-cm, respectively). These results provide strong justification that the contact metallization should not degrade after deposition of diamond films on Ti/Ni contact metallization useful for power electronic devices based on Si, SiC, and GaN semiconductors. Additional, research are planned on SiC and GaN substrates in support of the suggestion that no degradation should occur to Ti/Ni metallization on these wide band gap semiconductors useful for power electronics upon high temperature annealing and deposition in Ar or H_2 typically used in diamond film deposition.

4. Conclusions

We have demonstrated the influence of processing conditions on the Ti/Ni contact metallization on the p-Si (100) wafer for thermal management. Firstly, Ti/Ni films have been sequentially deposited on p-Si (100) substrates using the metal mask with circular vias by DC magnetron sputtering using separate pure Ti and Ni targets. The thickness of Ti was ~10 nm and of Ni ~1000 nm. Further, the contact resistance and electrical properties of metallized Ti/Ni film on Si were measured before and after annealing treatments in Ar and H_2 atmospheres at 380 °C for 1 h. The post annealing treatments in Ar and H_2 atmospheres led to better ohmic contacts and electrical properties such as resistivity, carrier concentration and Hall mobility. The typical resistivity values of 5-8 ohm-cm, carrier concentration of $\sim 1 \times 10^{22}$ /m^3, and Hall mobility of ~0.01–0.04 m^2/VS were obtained. These values are close to vendor supplied values for the Si (100) wafers (p-type, doping level of boron in Si (100) is 0.74×10^{21}–1.67×10^{22} m^{-3}. Also, mobility and resistivity are in the range of 0.0368–0.0418 m^2/V-S and 1-20 ohm-cm, respectively). The future research is focusing on the deposition of diamond on these metal layers and measure similar electrical properties and contact resistance of metallized semiconductors after diamond deposition as heat spreader. Current work in progress will include metallized Si, SiC and GaN substrates that are attractive for the present and future high power and microelectronic devices.

CRediT authorship contribution statement

Manish Singh: Data curation, Formal analysis, Investigation, Methodology, Validation, Writing – original draft. **Lakshmi Narayanan Ramasubramanian:** Data curation, Formal analysis, Methodology, Validation. **Raj N. Singh:** Conceptualization, Formal analysis, Funding acquisition, Investigation, Methodology, Project administration, Resources, Supervision, Writing – review & editing.

Declaration of Competing Interest

None of the authors have any conflicts or interests to declare

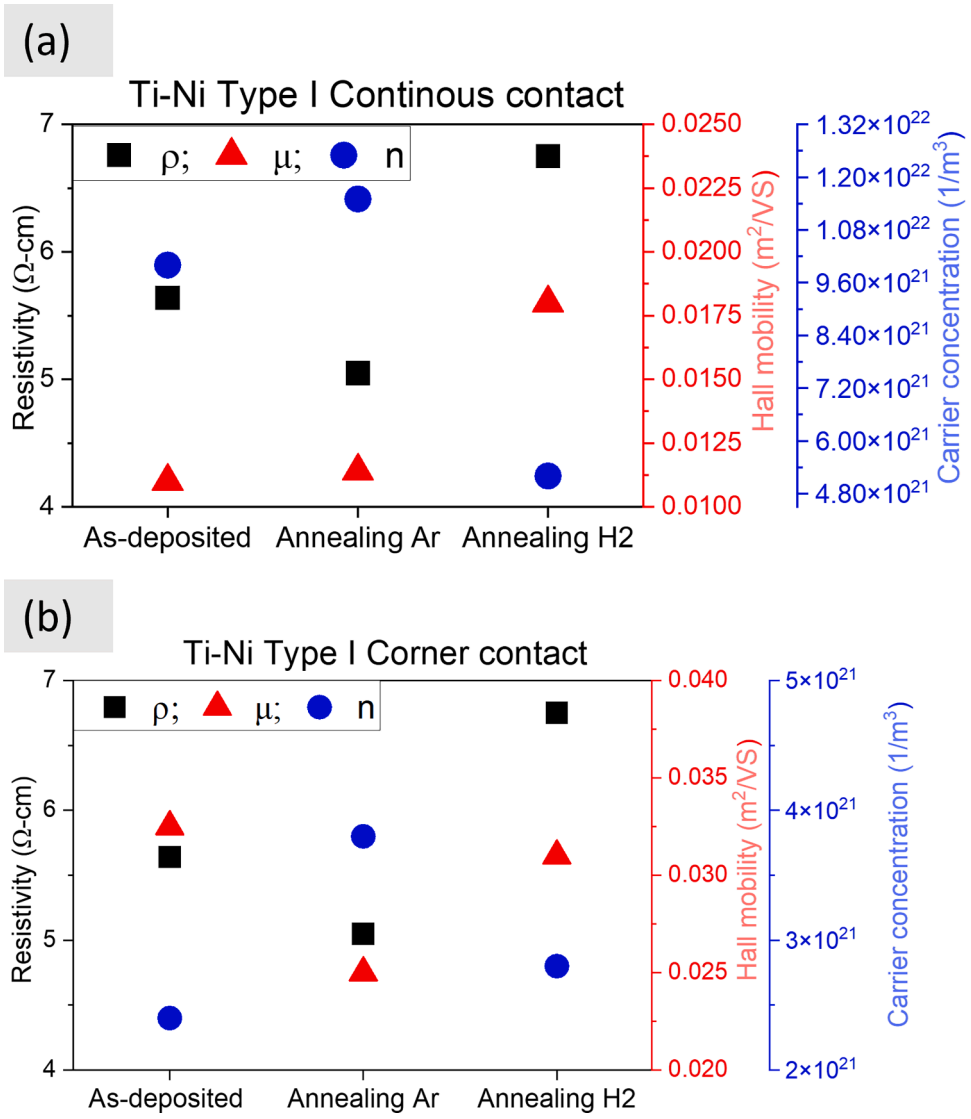

Fig. 9. The resistivity, carrier concentration, and Hall mobility of p-Si (100) in the as-deposited, annealed in Ar and annealed in H_2 at 380 °C for 1 h obtained from the (a) continuous contact dot-pattern and (b) corner contact dot-pattern of Ti/Ni metallization through Hall measurement.

Table 2
A summary of electrical properties of p-Si (100) obtained from Hall measurement using continuous and corner contacts of Ti/Ni metallization and effect of annealing in Ar and H_2 atmospheres at 380 °C for 1 h.

Ti/Ni Contact Processing Condition	Resistivity (ohm-cm)		Carrier concentration ($1/m^3$)		Hall mobility (m^2/VS)	
	Continuous	Corner	Continuous	Corner	Continuous	Corner
As deposited	5.64	8.45	1.0×10^{22}	0.24×10^{22}	0.0110	0.0325
Annealed in Ar	5.05	6.45	1.1×10^{22}	0.38×10^{22}	0.0114	0.0250
Annealed in H_2	6.75	7.60	0.52×10^{22}	0.28×10^{22}	0.0180	0.0310

Data availability

Data will be made available on request.

Acknowledgments

This research is based on work supported by the National Science Foundation under NSF Award Number 2122495. Any opinions, findings and conclusions or recommendations expressed in this material are those of the authors and do not reflect views of the national science foundation.

References

[1] Y. Fu, H. Du, W. Huang, S. Zhang, M. Hu, TiNi-based thin films in MEMS applications: a review, Sens. Actuators A Phys. 112 (2-3) (2004) 395–408.
[2] K. Mech, R. Kowalik, P. Żabiński, Cu thin films deposited by DC magnetron sputtering for contact surfaces on electronic components, Arch. Metall. Mater. 56 (4) (2011).
[3] X. Cao, X. Cao, Q. Zhang, Nanoscale indentation behavior of pseudo-elastic Ti–Ni thin films, J. Alloy. Compd. 465 (1-2) (2008) 491–496.
[4] J.A. Oke, T.C. Jen, Atomic layer deposition and other thin film deposition techniques: from principles to film properties, J. Mater. Res. Technol. 21 (2022) 2481–2514.

[5] M. Swain, D. Bhattacharya, K.G. Bhushan, S. Basu, Deposition of a nickel film by DC magnetron sputtering and its characterization, AIP Conf. Proc. 1451 (1) (2012) 182–184.

[6] M.C. Rao, M.S. Shekhawat, A brief survey on basic properties of thin films for device application, Int. J. Mod. Phys. Conf. Ser. 22 (2013) 576–582.

[7] H. Nienhaus, H.S. Bergh, B. Gergen, A. Majumdar, W.H. Weinberg, E. W. McFarland, Ultrathin Cu films on Si(111): schottky barrier formation and sensor applications, J. Vac. Sci. Technol. A 17 (4) (1999) 1683–1687.

[8] B.G. Priyadarshini, S. Aich, M. Chakraborty, Nano-crystalline Ni Ti alloy thin films fabricated using magnetron co-sputtering from elemental targets: effect of substrate conditions, Thin. Solid. Films 616 (2016) 733–745.

[9] B. Geetha Priyadarshini, S. Aich, M. Chakraborty, An investigation on phase formations and microstructures of Ni-rich Ni-Ti shape memory alloy thin films, Metall. Mater. Trans. A 42 (11) (2010) 3284–3290.

[10] V. Chawla, R. Jayaganthan, A.K. Chawla, R. Chandra, Morphological study of magnetron sputtered Ti thin films on silicon substrate, Mater. Chem. Phys. 111 (2-3) (2008) 414–418.

[11] L. Adnane, A. Gokirmak, H. Silva, High temperature Hall measurement setup for thin film characterization, Rev. Sci. Instrum. 87 (7) (2016), 075117.

[12] J.M.E. Harper, K.P. Rodbell, Microstructure control in semiconductor metallization, J. Vac. Sci. Technol. B 15 (4) (1997) 763–779.

[13] P.C. Andricacos, C. Uzoh, J.O. Dukovic, J. Horkans, H. Deligianni, Damascene copper electroplating for chip interconnections, IBM J. Res. Dev. 42 (5) (1998) 567–573.

[14] C.H. Jo, N. Voronina, S.T. Myung, Single-crystalline particle Ni-based cathode materials for lithium-ion batteries: Strategies, status, and challenges to improve energy density and cyclability, Energy Stor. Mater. 51 (2022) 568–587.

[15] F. Schlichting, L. Thormählen, J. Cipo, D. Meyners, H. Kersten, Energy-dependent film growth of Cu and NiTi from a tilted DC magnetron sputtering source determined by calorimetric probe analysis, Surf. Coat. Technol. 450 (2022).

[16] B.G. Priydarshini, N. Esakkiraja, S. Aich, M. Chakraborty, Resputtering effect on nanocrystalline Ni-Ti alloy films, Metall. Mater. Trans. A 47 (4) (2016) 1751–1760.

[17] P. Krulevitch, A.P. Lee, P.B. Ramsey, J.C. Trevino, J. Hamilton, M.A. Northrup, Thin film shape memory alloy microactuators, J. Microelectromech. Syst. 5 (4) (1996) 270–282.

[18] X. Bai, Q. Cai, W. Xie, Y. Zeng, C. Chu, X. Zhang, In-situ crystalline TiNi thin films deposited by HiPIMS at a low substrate temperature, Surf. Coat. Technol. 455 (2023), 129196.

[19] S. Miyazaki, A. Ishida, Martensitic transformation and shape memory behavior in sputter-deposited TiNi-base thin films, Mater. Sci. Eng. A 273-275 (1999) 106–133.

[20] H. Cho, H.Y. Kim, S. Miyazaki, Fabrication and characterization of Ti–Ni shape memory thin film using Ti/Ni multilayer technique, Sci. Technol. Adv. Mate 6 (6) (2005) 678–683.

[21] N. Govindaraju, R.N. Singh, Effect of microwave plasma process conditions on nanocrystalline diamond deposition on AlGaN/GaN HEMT and Si device metallizations. Ceramic Transactions 234, 2012. https://doi.org/10.1002/9781118491867.ch12. Citations: 2.

[22] N. Govindaraju, R.N. Singh, Processing of nanocrystalline diamond thin films for thermal management of wide-bandgap semiconductor power electronics, Mater. Sci. Eng. B 176 (14) (2011) 1058–1072.

[23] N. Govindaraju, C. Kane, R.N. Singh, Processing of multilayer microcrystalline and nanocrystalline diamond thin films using Ar-rich microwave plasmas, J. Mater. 26 (2011) 3072–3082.

[24] N. Govindaraju, R.N. Singh, Theoretical consideration of the parameter space for thermal conductivity measurements of thin diamond films, Comput. Mater. Sci. 43 (3) (2008) 423–439.

[25] N. Govindaraju, D. Das, R.N. Singh, P.B. Kosel, High-temperature electrical behavior of nanocrystalline and microcrystalline diamond films, J. Mater. 23 (10) (2008) 2774–2786.

[26] D. Das, R.N. Singh, A review of nucleation, growth and low temperature synthesis of diamond thin films, Int. Mater. Rev. 52 (2007) 29–64.

[27] D. Das, R.N. Singh, S. Chattopadhyay, H.H. Chen, Thermal conductivity of diamond films deposited at low surface temperatures, J. Mater. Sci. Res. 21 (9) (2006) 2379–2388.

[28] M. Seelmann-Eggebert, P. Meisen, F. Schaudel, P. Koidl, A. Vescan, H. Leier, Heat-spreading diamond films for GaN-based high-power transistor devices, Diam. Relat. Mater. 10 (3) (2001) 744–749.

[29] S. Kyatam, D. Mukherjee, H. Neto, J.C. Mendes, Thermal management of photonic integrated circuits: impact of holder material and epoxies, Appl. Opt. 58 (22) (2019) 6126–6135.

[30] J.E. Graebner, S. Jin, G.W. Kammlott, Y.H. Wong, J.A. Herb, C.F. Gardinier, Thermal conductivity and the microstructure of state-of-the-art chemical-vapor-deposited (CVD) diamond, Diam. Relat. Mater. 2 (5) (1993) 1059–1063.

[31] S. Kyatam, D. Mukherjee, A. Silva, L. Alves, S. Rotter, M. Neto, F. Oliveira, R. Silva, H. Neto, J.C. Mendes, CVD diamond films for thermal management applications, in: Proceedings of the IEEE International Conference on Microwaves, Antennas, Communications and Electronic Systems (COMCAS), 2019, pp. 1–6.

[32] J. Van Der Pauw L, A method of measuring the resistivity and Hall coefficient on lamellae of arbitrary shape, PhiTR 20 (1958) 220–224.

[33] L. Pauw, A method of measuring specific resistivity and Hall effect of discs of arbitrary shape, Philips Res. Rep. 13 (1) (1958) 1–9.

[34] W.S. Liu, Y.L. Chang, C.Y. Tan, C.T. Tsai, H.C. Kuo, Properties of N-Type GaN thin film with Si-Ti codoping on a glass substrate, Crystals 10 (7) (2020).

[35] R. Kumar, S. Chand, Fabrication and electrical characterization of nickel/p-Si Schottky diode at low temperature, Solid State Sci. 58 (2016) 115–121.

[36] J.O. Olowolafe, M.A. Nicolet, J.W. Mayer, Influence of the nature of the Si substrate on nickel silicide formed from thin Ni films, Thin. Solid. Films 38 (2) (1976) 143–150.

[37] K.N. Tu, W.K. Chu, J.W. Mayer, Structure and growth kinetics of Ni2Si on silicon, Thin. Solid. Films 25 (2) (1975) 403–413.

[38] H. Kotake, Y. Oana, I. Watanabe, The diffusion barrier effect of a vanadium layer in the formation of nickel silicides, Thin. Solid. Films 75 (3) (1981) 247–252.

[39] M.A. Nicolet, Diffusion barriers in thin films, Thin. Solid. Films 52 (3) (1978) 415–443.

[40] M. Muhlbacher, G. Greczynski, B. Sartory, N. Schalk, J. Lu, I. Petrov, J.E. Greene, L. Hultman, C. Mitterer, Enhanced $Ti_{0.84}Ta_{0.16}N$ diffusion barriers, grown by a hybrid sputtering technique with no substrate heating, between Si(001) wafers and Cu overlayers, Sci. Rep. 8 (1) (2018) 5360.

[41] S.Q. Wang, I. Raaijmakers, B.J. Burrow, S. Suthar, S. Redkar, K.B. Kim, Reactively sputtered TiN as a diffusion barrier between Cu and Si, J. Appl. Phys. 68 (10) (1990) 5176–5187.

[42] P. Bhatt, A. Sharma, S.M. Chaudhari, Correlation of structural, chemical, and magnetic properties in annealed Ti/Ni multilayers, J. Appl. Phys. 97 (4) (2005).

[43] T. Lehnert, S. Tixier, P. Böni, R. Gotthardt, A new fabrication process for Ni–Ti shape memory thin films, Mater. Sci.Eng. A 273-275 (1999) 713–716.

[44] P. Bhatt, V. Ganeshan, V.R. Reddy, S.M. Chaudhari, High temperature annealing effect on structural and magnetic properties of Ti/Ni multilayers, Appl. Surf. Sci. 253 (5) (2006) 2572–2580.